Enhanced chiller sensor fault detection, diagnosis and estimation using wavelet analysis and principal component...

Article *in* Applied Thermal Engineering · February 2008

DOI: 10.1016/j.applthermaleng.2007.03.021

CITATIONS
56

READS
2,026

3 authors:

Xinhua Xu

53 PUBLICATIONS **1,021** CITATIONS

SEE PROFILE

Linda F. Xiao

The Hong Kong Polytechnic University

99 PUBLICATIONS **1,820** CITATIONS

SEE PROFILE

Shengwei Wang

The Hong Kong Polytechnic University

263 PUBLICATIONS **5,539** CITATIONS

SEE PROFILE

Available online at www.sciencedirect.com
ScienceDirect
Applied Thermal Engineering 28 (2008) 226–237
APPLIED THERMAL ENGINEERING
www.elsevier.com/locate/apthermeng

Enhanced chiller sensor fault detection, diagnosis and estimation using wavelet analysis and principal component analysis methods

Xinhua Xu, Fu Xiao, Shengwei Wang *

Department of Building Services Engineering, The Hong Kong Polytechnic University, Kowloon, Hong Kong

Received 7 February 2007; accepted 9 March 2007
Available online 24 March 2007

Abstract

An enhanced sensor fault detection, diagnosis and estimation (FDD&E) strategy is developed for centrifugal chillers using wavelet analysis method and principal component analysis (PCA) method. A number of sensors of concern in chiller system monitoring and control are assigned into a PCA model, which can group these correlated variables and capture the systematic variations of chillers. Raw measurements or simple processing measurements of sensors may deteriorate the performance of sensor FDD&E strategy using PCA because of the embodied noises and dynamics. Wavelet analysis can extract the approximations of sensor measurements by separating noises and dynamics. Using these approximation coefficients for PCA modeling we can improve the capability and reliability of fault detection and diagnosis as well as the accuracy of sensor fault estimation. This wavelet–PCA-based sensor FDD&E strategy was validated using field operation data of an existing centrifugal chiller plant while various sensor faults of different magnitudes were introduced. The results demonstrate that this strategy can produce better performance of sensor FDD&E in terms of fault detection ratio, diagnosis ratio and estimation accuracy by comparing with conventional PCA-based sensor FDD&E strategy using raw or simple processing measurements for PCA modeling.

Keywords: Centrifugal chiller; Sensor fault; Fault detection and diagnosis and estimation; Wavelet analysis; Approximation coefficients; Principal component analysis

1. Introduction

Chillers are widely used nowadays in various buildings. Their performance is affected by the ever changing operating conditions, and the performance degrades naturally. Optimal and robust control benefits by improving operation, prolonging life and saving energy [3,4,6,11,28]. On the other hand, different kinds of faults may occur in chiller systems, resulting in excessive energy consumption, complaints from occupants and shorten equipment life, etc. The applications of fault detection and diagnosis (FDD) are essentially important to ensure that these systems operate properly and consume energy efficiently. The main benefits of FDD in HVAC&R applications are derived mainly from reduced energy consumption and operation costs and/or improved indoor environment. Various FDD strategies and methods, addressing common faults in chiller system and its components to improve operation, have been presented by Grimmelius and Woud [12], Stylianou [24], Rossi and Braun [21], Jia and Reddy [14] and Cui and Wang [8], etc.

Reliability and accuracy of sensor measurements is essential to performance monitoring, implementation of optimal control strategies and component and system performance FDD. Sensor FDD has been considered very seriously in a few fields, such as (nuclear) power plant, chemical engineering, etc. [10]. The methods of sensor FDD can be roughly grouped into two categories: model-free methods and model-based methods. Limit checking [17], physical redundancy [19], intelligent instruments [7],

* Corresponding author. Tel.: +852 27730345; fax: +852 27746146.
E-mail address: beswwang@polyu.edu.hk (S. Wang).

1359-4311/$ - see front matter © 2007 Elsevier Ltd. All rights reserved.
doi:10.1016/j.applthermaleng.2007.03.021

Nomenclature

A	matrix
$a(n)$	approximation coefficients
B	matrix of approximation coefficients
b	dilation (scaling) parameter, integer
C	specific heat of water
Cov	covariance matrix
CWT	continuous wavelet transfer
DWT	discrete wavelet transfer
$d(n)$	detail coefficients
Eff	efficiency
Err	relative estimation error
e	residual vector
Hi_D	high-pass analysis filter
Hi_R	high-pass synthesis filter
h	specific enthalpy of refrigerant
I	unit matrix
LMTD	logarithm mean temperature difference
Lo_D	low-pass analysis filter
Lo_R	low-pass synthesis filter
l,m,n	integer
M	water flow rate
P	principal load matrix, pressure
Q_α	threshold
Q_{loss}	heat loss
SPE	squared prediction error
T	temperature
t	time
τ	translation (shift) parameter
U	matrix
v	specific volume of refrigerant
W	power input
WT	wavelet transfer
x	signals
$Y^{n\times m}$	sample matrix involving n observation and m process variables
y	observation vector
$\bar{y}$	estimation of faulty y

Greeks

ψ	mother wavelet
ψ^*	conjugate function of a mother wavelet
Λ	diagonal matrix
β_i	detected fault direction
γ	mean isentropic coefficient of refrigerant
η_i	contribution of the ith variable to the total sum of variations

Superscripts

$1,2,n$	integer

Subscripts

1,2	state points in pressure–enthalpy graph
cd	condenser or condensing
chw	chilled water
chws	chilled water supply
chwr	chilled water return
comp	compressor
cw	condensing water
cwr	condensing water return
cws	condensing water supply
ev	evaporator

etc. are typical model-free methods. In HVAC field, model-based methods are often used for sensor fault detection and diagnosis. These methods mainly involve the physical model [26], the ARX/RARX model [32], the neural network model [16,25], the principal component analysis (PCA) model [15,27], and so forth.

The PCA model is used to capture the major normal statistical correlation among the measurements of system variables on the basis of training data in normal operation, and to generate the residuals that quantify the main variances. The residuals are usually some kind of statistics, which can be used to detect and diagnose faults. In air conditioning system, a sensor FDD strategy based on PCA model was developed to diagnose the flow rate sensors of VAV box [29]. Wang and Cui [30] used the PCA model to develop a strategy for diagnosing the measurements of a centrifugal chiller, and then estimating the real measurement if faulty. The data used for model training or to be diagnosed normally go through a steady-state filter to filter out the data of significant dynamics [30]. Moving average is also often used to reduce noises. However, the remaining noises and dynamics embodied in the measured data usually deteriorate the performance of PCA for fault diagnosis resulting in low sensitivity to sensor faults. The accuracy and reliability of the reconstruction of faulty sensors using PCA method are reduced when the data with remaining noise and dynamic are used.

Wavelet analysis, also called wavelet transform, is a kind of variable window technology, which uses a shorter time interval to analyze the high frequency components of a signal and a longer one to analyze the low frequency components of the signal [2,23]. The raw data using wavelet transform can be decomposed into detail coefficients and approximation coefficients in a multiscale. The noise and events associated with the sensor' normal behaviors responding to dynamic change appear clearly in the finer scales represented with detail coefficients. The events of sensor drift, bias, etc. appear most strongly in the coarser scales represented with approximation coefficients. That means the approximation coefficients can represent the characteristics of faulty sensors by separating the noise and dynamics. Many studies present the applications of

wavelet analysis to decompose signals for improving the performance of sensor fault detection and diagnosis in industrial fields [5,9,31,33].

This paper presents a robust sensor fault detection and diagnosis and estimation (FDD&E) strategy for a typical chiller system. This strategy employs wavelet analysis and PCA analysis methods. Wavelet analysis is used to extract the approximations of the sensor measurements involved in a typical chiller system by separating noises and dynamics. The PCA method is used to establish the normal statistical correlation among the approximations of the sensor measurements to detect, diagnose and estimate sensor faults. Field operation data from a real-world centrifugal chiller system are used to evaluate the capability and performance of this strategy for chiller sensor fault detection and diagnosis and estimation. This wavelet–PCA-based chiller sensor FDD&E strategy and validation are presented in this paper by comparing with conventional PCA-based chiller sensor FDD&E strategy using raw operation data or simple processing measurements for PCA modeling directly.

2. Principle of wavelet analysis

Wavelet analysis is a kind of variable window technology, which uses a shorter time interval to analyze the high frequency components of a signal and a longer time interval to analyze the low frequency components of the signal [23]. It has favorable local time-frequency characteristics. Wavelet transform (WT) includes continuous wavelet transform (CWT) and discrete wavelet transform (DWT).

The continuous wavelet transform of signal x is to perform the convolution operation of this signal and a basic function as Eq. (1). For most practical applications, the wavelet coefficients are discretized dyadically by a factor of $2^m n$ for shift and by a factor of 2^m for scaling. The above equation is then expressed as Eq. (2) as follows.

$$\mathrm{WT}_x(b,\tau) = \frac{1}{\sqrt{b}} \int x(t)\psi^*\left(\frac{t-\tau}{b}\right) \mathrm{d}t \tag{1}$$

$$\mathrm{WT}_x(m,n) = 2^{-\frac{m}{2}} \int x(t)\psi^*(2^{-m}t - n)\,\mathrm{d}t \tag{2}$$

where, $\psi^*(t)$ is the conjugate function of the mother wavelet $\psi(t)$, b and τ are the dilation (scaling) and translation (shift) parameters, respectively, m and n are integers.

The discrete wavelet transform is found to yield a fast computation of the wavelet transform. It is computed by a successive low pass and high pass filtering of the discrete digital signal as shown in Fig. 1a, and the inverse DWT is to reconstruct the signal based on the coincident multilevel wavelet decomposition as shown in Fig. 1b. They are called the Mallat algorithm. Its significance is that it connects the continuous time multi-resolution to the discrete time filters. These filters are generated using wavelets.

In the wavelet decomposition process, as shown in Fig. 1a, the algorithm operates by applying the low-pass analysis filter (Lo_D) and high-pass analysis filter (Hi_D)

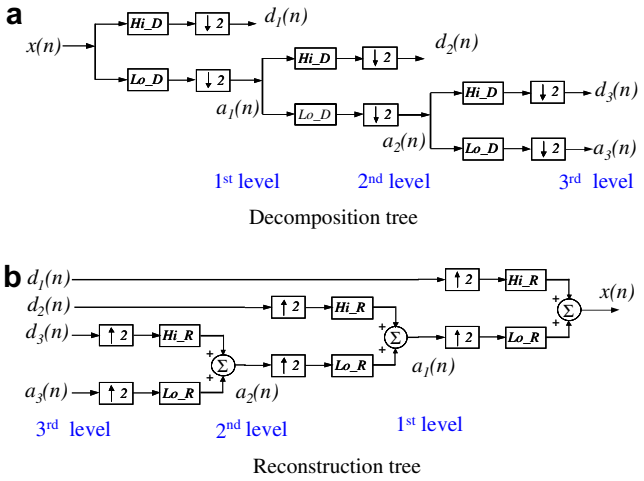

Fig. 1. Schematics of three level wavelet decomposition and reconstruction.

on the original signal ($x(n)$) resulting in approximation coefficients ($a(n)$) and detail coefficients ($d(n)$), respectively, together with down sampling. Down sampling halves the number of samples at each iteration. The procedure repeats on the resulted approximation coefficients to obtain the approximation coefficients and detail coefficients at the next level. The vectors of detail coefficients are the detail of the signal lost when moving from an approximation at one level to the next courser level. In the wavelet reconstruction process, as shown in Fig. 1b, the algorithm operates by applying the low-pass synthesis filter (Lo_R) and high-pass synthesis filter (Hi_R) on the approximation coefficients ($a(n)$) and detail coefficients ($d(n)$), respectively, together with up sampling, resulting in the approximation coefficients at the low level. The procedure repeats until the original signal is obtained. Up-sampling operation is to double the number of samples at each iteration.

Approximation coefficients are the low frequency coefficients which describe the trend or the approximation of a signal. The approximation coefficients at the high level are more smoother than that at the low level. Detail coefficients are the high frequency coefficients which describe the details of a signal, i.e., the transient of a signal. As for the measurements of sensors analyzed using multiscale wavelet decomposition, the noises and the events associated with the sensor's normal behaviors responding to input change will appear clearly in the finer scale representing with detail coefficients. When a bias or drift occurs, the event will appear strongly in the coarser scales represented with approximation coefficients. Fig. 2 presents the detail coefficients and approximate coefficients of a series of normal return chilled water temperature using level 1 wavelet decomposition. When this series was introduced with a bias (2 °C), it was also decomposed into detail coefficients and approximate coefficients as shown in the figure. It is obvious that the detail coefficients of both the normal data series and the faulty data series are identical while the approximate coefficients of both series are different. This

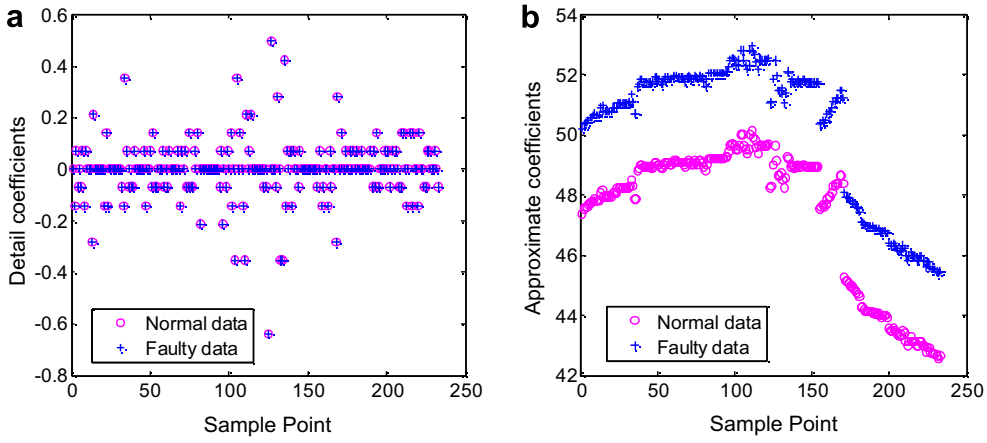

Fig. 2. Level 1 wavelet decomposition of data series.

means the faulty information is totally represented by these approximate coefficients. Therefore, these approximation coefficients can be used to establish the PCA model to improve sensor fault detection, diagnosis and estimation.

3. Wavelet–PCA-based chiller sensor FDD&E strategy

3.1. A brief review on the PCA method in sensor FDD&E applications

Principal component analysis (PCA) is a multivariate analysis technique, also a dimension reduction technique. It produces a lower dimensional representation in a way that preserves the correlation structure among the process variables [22]. Using the PCA method, a sample matrix ($Y^{n\times m}$) involving n observation and m process variables representing normal process is decomposed into principal component subspace and residual subspace. The principal component subspace represents the correlation of these process variables. It is represented with a principal load matrix P ($P \in R^{m\times l}$), i.e., a space consisting of the eigenvectors corresponding to the $l(l < m)$ largest eigenvalues which is determined by the eigenvalue decomposition of the covariance matrix as Eq. (3). When a new observation vector y is projected to the principal component space, the residual vector (e) can be calculated as Eq. (4). This residual can describe the variation and noise of the new observation, and is the basis for FDD&E.

$$\mathrm{Cov} = Y^{\mathrm{T}}Y/(n-1) = U\Lambda U^{\mathrm{T}} \tag{3}$$

$$e = y(I - PP^{\mathrm{T}}) \tag{4}$$

where Cov is the covariance matrix, Λ is a diagonal matrix of non-negative real eigenvalues, U is a matrix whose columns are the corresponding eigenvectors, I is unit matrix.

With respect to the FDD applications of PCA, Q-statistic as Eq. (5) is used as an index of faulty conditions. It is also known as squared prediction error (SPE). When no fault exists, the Q-statistic is less than a threshold (Q_α), representing the normal dynamic and measurement noise, etc. of the measurements. On the contrary, when faults exist, the correlations among the measurements of the variables is destroyed, the Q-statistic is larger than the threshold. At this moment, the faulty sensor can be diagnosed in terms of Q-contribution as Eq. (6), and is estimated as Eq. (7) by minimizing the squared prediction error of reconstructed vector of variables.

$$Q\text{-statistic} = \mathrm{SPE} = e^{\mathrm{T}}e = \|y(I - PP^{\mathrm{T}})\|^2 \leqslant Q_\alpha \tag{5}$$

$$\eta_i = \frac{\|e_i\|^2}{Q\text{-statistic}} \tag{6}$$

$$\bar{y} = y(I - \beta_i^{\mathrm{T}}\beta_i(I - PP^{\mathrm{T}})/\|\beta_i(I - PP^{\mathrm{T}})\|^2) \tag{7}$$

where Q_α is the threshold statistically determined according to the measurements of the training matrix [13], e_i presents the ith element of the residual vector e and η_i is the contribution of the ith variable to the total sum of variations in the residual space (i.e., the Q-statistic), $\bar{y}$ is the estimation of faulty y, β_i is the detected fault direction. For example, $\beta_1 = [1, 0, 0, 0, \ldots, 0]$ means there is fault associated with the first variable in an observation.

3.2. PCA model of chiller system

Fig. 3a illustrates the main components and instrumentations of a typical water-cooled centrifugal chiller system, and Fig. 3b is the schematics of the pressure–enthalpy diagram of this refrigeration cycle. This system involves four major components: evaporator, compressor, condenser and throttle valve. The heat of the building is taken away by chilled water and then transferred to a refrigerant of a low temperature and pressure in the evaporator. The refrigerant vapor in the evaporator is pumped by the compressor to the condenser with high pressure and high temperature. The vapor of high temperature and high pressure condenses by rejecting the heat to the cooling water which is subsequently cooled down by cooling towers. The liquid refrigerant of high temperature and high pressure is expanded through the throttle valve into low temperature and low pressure. Then the refrigeration cycle repeats.

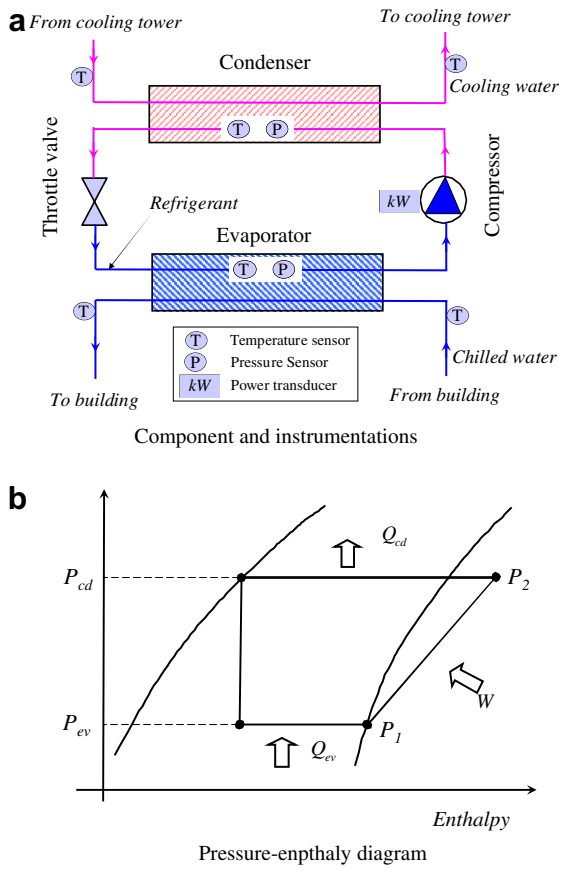

Fig. 3. Schematic of a typical centrifugal chiller refrigeration cycle.

For chiller monitoring and control, lots of sensors are implemented. The most essential instrumentations existing in most chiller systems are shown in Fig. 3a. These measurements are supply chilled water temperature (T_{chws}), return chilled water temperature (T_{chwr}), evaporating temperature (T_{ev}), evaporating pressure (P_{ev}), compressor power input (W_{comp}), supply cooling water temperature (T_{cws}), return cooling water temperature (T_{cwr}), condensing temperature (T_{cd}), condensing pressure (P_{cd}). In most chiller systems, the water flow rates in the evaporator (M_{chw}) and condenser (M_{cw}) are constant to ensure the safe operation of chillers. The water flow meters are not often provided.

The PCA model in this study involves the above nine variables only. Matrix **A** ($n \times 9$) represents the original matrix with n samples of these variables as follows:

$$\mathbf{A} = \begin{bmatrix} T^1_{chws} & T^1_{chwr} & T^1_{cws} & T^1_{cwr} & T^1_{ev} & T^1_{cd} & P^1_{ev} & P^1_{cd} & W^1_{comp} \\ T^2_{chws} & T^2_{chwr} & T^2_{cws} & T^2_{cwr} & T^2_{ev} & T^2_{cd} & P^2_{ev} & P^2_{cd} & W^2_{comp} \\ \cdots & \cdots & \cdots & \cdots & \cdots & \cdots & \cdots & \cdots & \cdots \\ T^n_{chws} & T^n_{chwr} & T^n_{cws} & T^n_{cwr} & T^n_{ev} & T^n_{cd} & P^n_{ev} & P^n_{cd} & W^n_{comp} \end{bmatrix} \quad (8)$$

The strong correlations among the variables in matrix **A** can be explained as follows. For a specific chiller system with constant chilled water and cooling water flow rates, the temperatures of chilled water (T_{chws}, T_{chwr}) as well as the supply cooling water temperature (T_{cws}) are the determinant variables for operating conditions and performance of a centrifugal chiller [1,18]. Clearly, these three deterministic variables, i.e., T_{chws}, T_{chwr} and T_{cws}, are included in matrix **A**. At the same time, the variables in the matrix jointly determine the performance of chillers as indicated in Eqs. (9)–(11).

$$\mathrm{Eff}_{comp} = \frac{\gamma P_1 v_1 [(P_2/P_1)^{(\gamma-1)/\gamma} - 1]}{(\gamma - 1)(h_2 - h_1)} \quad (9)$$

$$\mathrm{LMTD}_{ev} = \frac{T_{chwr} - T_{chws}}{\ln\left(\frac{T_{chwr} - T_{ev}}{T_{chws} - T_{ev}}\right)} \quad (10)$$

$$\mathrm{LMTD}_{cd} = \frac{T_{cwr} - T_{cws}}{\ln\left(\frac{T_{cwr} - T_{cd}}{T_{cws} - T_{cd}}\right)} \quad (11)$$

where, Eff_{comp} is the efficiency of compression process, LMTD_{ev} and LMTD_{cd} are the logarithm mean temperature differences of the evaporator and condenser, respectively. The energy input to compressor (W_{comp}) essentially depends on the Eff_{comp}, consequently is determined by P_1 and P_2. T_{ev} and T_{cd} are evaporating and condensing temperatures which correspond to P_{ev} and P_{cd}, respectively. v_1 is the specific volume of refrigerant at the inlet of compressor and determined by the evaporating pressure and temperature, γ is the mean isentropic coefficient of refrigerant, P_2 is the refrigerant pressure at compressor outlet (approximately represented with condensing pressure P_{cd}) and P_1 is the refrigerant pressure at compressor inlet (approximately represented with evaporating pressure P_{ev}), h_1 is the specific enthalpy of the refrigerant at compressor inlet which can be approximately determined using evaporating pressure and temperature (saturated), h_2 is the specific enthalpy of the refrigerant at compressor outlet which can be approximately determined using condensing pressure and temperature (saturated).

In addition, due to energy balance of the chiller under steady state, there are strong correlations among these seven variables: W_{comp}, M_{chw}, T_{chws}, T_{chwr}, M_{cw}, T_{cws} and T_{cwr}, as Eq. (12). In a certain range of operating conditions, the heat loss (Q_{loss}) can be assumed constant.

$$W_{comp} + M_{chw} C_{pw} (T_{chwr} - T_{chws}) - M_{cw} C_{pw} (T_{cwr} - T_{cws}) + Q_{loss} = 0 \quad (12)$$

According to the above analysis, it might be concluded that all the variables in matrix **A** are strongly correlated with each other from a perspective of thermophysics, and the correlations might be captured by the PCA method.

3.3. Structure of wavelet–PCA-based chiller sensor FDD&E strategy

The wavelet–PCA method is different from the conventional PCA method. PCA model in time domain uses the raw or simple processing training data and observation

samples for PCA modeling and analysis directly (*For concise description, this PCA model is called the conventional PCA model*). The simple data processing includes filtering obvious outliers and employing steady-state filter, etc. However, these processed data still embody a large amount of noises and dynamics. Wavelet–PCA method first decomposes the training data or observation samples to the approximation of these data by separating the noise and dynamics to some extent. Then this method uses the approximations for PCA modeling and data analysis. The matrix $(n' \times 9)$ of approximation coefficients **B** decomposed from Matrix **A** is as follows:

$$B = \begin{bmatrix} a^1_{T_{\text{chws}}} & a^1_{T_{\text{chwr}}} & a^1_{T_{\text{cws}}} & a^1_{T_{\text{cwr}}} & a^1_{T_{\text{ev}}} & a^1_{T_{\text{cd}}} & a^1_{P_{\text{ev}}} & a^1_{P_{\text{cd}}} & a^1_{W_{\text{comp}}} \\ a^2_{T_{\text{chws}}} & a^2_{T_{\text{chwr}}} & a^2_{T_{\text{cws}}} & a^2_{T_{\text{cwr}}} & a^2_{T_{\text{ev}}} & a^2_{T_{\text{cd}}} & a^2_{P_{\text{ev}}} & a^2_{P_{\text{cd}}} & a^2_{W_{\text{comp}}} \\ \cdots & \cdots & \cdots & \cdots & \cdots & \cdots & \cdots & \cdots & \cdots \\ a^{n'}_{T_{\text{chws}}} & a^{n'}_{T_{\text{chwr}}} & a^{n'}_{T_{\text{cws}}} & a^{n'}_{T_{\text{cwr}}} & a^{n'}_{T_{\text{ev}}} & a^{n'}_{T_{\text{cd}}} & a^{n'}_{P_{\text{ev}}} & a^{n'}_{P_{\text{cd}}} & a^{n'}_{W_{\text{comp}}} \end{bmatrix} \quad (13)$$

where a are the approximation coefficients.

Fig. 4 illustrates the structure of the wavelet–PCA-based chiller sensor FDD&E strategy. This structure involves two parts. One is the development and training of the wavelet–PCA model. The other is online chiller sensor fault detection and diagnosis and estimation based on the trained model. The wavelet–PCA model is developed and trained prior to the implementation of the FDD&E applications.

Five steps are mainly involved in the development and training of the wavelet–PCA model, i.e., data preprocessing, wavelet decomposition, decomposition of covariance matrix, determination of principal component (PC) subspace and calculation of the threshold of Q-statistic. Data preprocessing is to filter out the obvious outliers and to filter out the data of significant dynamics using a steady-state filter. Wavelet decomposition is to decompose the preprocessed data into approximation coefficients by separating noise and dynamics. These approximation coefficients are normalized to construct the training data matrix (measurement space) to avoid the effects of the units in the original data. The covariance matrix is decomposed to determine how many PCs are retained for the PC subspace. Jackson [13] suggested many commonly used criteria for choosing PCs. The PC subspace and the threshold of Q-statistic are used for the subsequent FDD&E of the sampling observations.

The FDD&E process also involves data preprocessing, wavelet decomposition. The approximation coefficient is projected to the residual subspace to calculate the residual for Q-statistic to detect if a fault occurs by comparing with the threshold determined in the modeling process. When the Q-statistic goes beyond the threshold, Q-contribution plot is used to diagnose as to which sensor is faulty. Generally, the larger the contribution of a variable makes to the Q-statistic, the higher the possibility of a fault in that

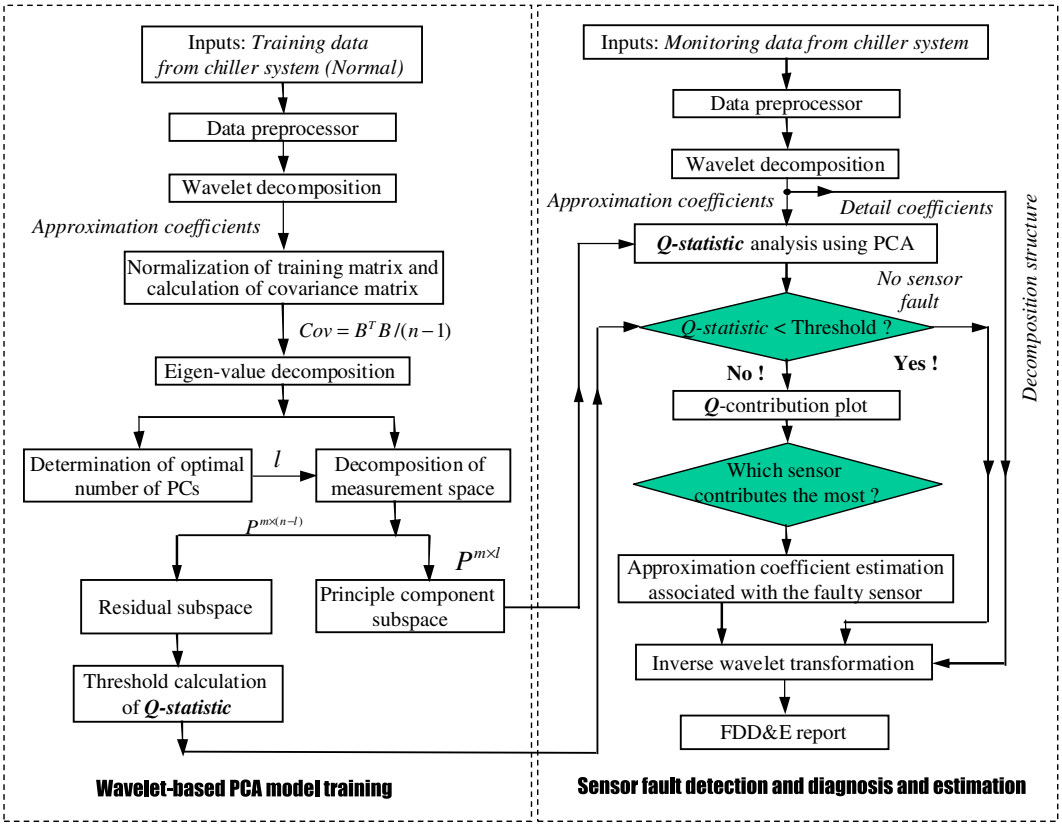

Fig. 4. Structure of the wavelet–PCA-based chiller sensor FDD&E strategy.

variable. When the faulty sensor is diagnosed, the approximation coefficient associated with the faulty sensor is estimated as Eq. (7). The estimated approximation coefficient and the detail coefficient are used to reconstruct the real measurement of this sensor together with the decomposition structure. Finally, the FDD&E result is reported.

4. Strategy validation using a real chiller system

4.1. Description of chiller system

This strategy was validated using the field site operation data of a chiller plant. This chiller plant serving a high-rising complex in Hong Kong involves three identical 1540-ton centrifugal chillers for day mode and two identical 500-ton centrifugal chillers for night/holiday mode. These chillers are cooled down by cooling water using cooling towers. The water flow rates through condensers and evaporators are all constant. The chilled water and cooling water flow rates, water temperatures, evaporating and condensing pressures, evaporating and condensing temperatures, compressor power of each chiller are collected at the interval of one minute from the built-in control panels of the chillers integrating with the BMS. These measurements can be retrieved from BMS database.

Temperatures are measured by resistance thermometers of accuracy ±0.05 °C. Water flow rate is measured by the electromagnetic flow meter with accuracy ±1% of the full range. Electric powers of individual chiller are measured using three-phase power transducers of accuracy ±0.5% of the full scale. Evaporating and condensing pressures are measured by pressure transducers with the accuracy 0.4% of the respective full working ranges.

The measurements of chillers in a summer month (July) were retrieved from the BMS database to validate the wavelet–PCA-based chiller sensor FDD&E strategy. The chiller plant operated throughout the day. The data on the fourth day were used to train models since the operation of the chiller plant was guaranteed to be normal and fault-free after this plant had just gone through routine maintenance. The data from each of the following days were used to generate faulty data by adding biases. Many validation tests were conducted using the generated data to test the faulty detectability and isolability of this strategy. For conciseness, only the test results using the operation data of one 1540-ton chiller on the fifth day are presented in this study. The operation conditions on this day did not vary significantly from the previous day.

4.2. Data processing

Since the PCA methods are based on steady-state operation of chiller system, all the data for model training and model validation must go through an outlier detector and a steady-state filter to rule out the data with significant dynamics. In this study, the steady-state filter is designed based on moving slope estimation of variables of concern [20]. However, these remaining data still embody obvious noise and dynamics. Wavelet decomposition is further used to process these data to separate obvious noise and dynamics for analysis.

For discrete wavelet transfer, the minimum continuous data points for decomposition are 2^n when the decomposition level is n. In this study, level-3 decomposition is employed to extract the approximation coefficients for model training and model validation of the wavelet–PCA-based chiller sensor FDD&E strategy. Therefore, these data after filtering are further processed to meet the requirement of discrete wavelet decomposition by ruling out the discontinuous data points. A set of continuous data points is a data group.

The number of the original samples for model training under normal sensor conditions was 851. After filtering and processing, 217 samples of 15 groups remained for wavelet decomposition to develop the wavelet–PCA model. For model validation case, 243 samples of 10 groups out of 890 original samples remained to validate the wavelet–PCA model for sensor FDD&E. It is worth to point out that the same number of samples was used directly to develop the conventional PCA model without data transform for performance comparison.

4.3. Training of models

With respect to the training matrix **A**, three principal components corresponding to the three largest eigenvalues could explain 97.6% of the total variance of the system. These three PCs were retained in the PCA model. The detection threshold of Q-statistics of 95% confidence level was calculated to be 0.9065. The Q-statistics plot of the conventional PCA model using the measurement directly in normal sensor conditions is illustrated as Fig. 5. The Q-statistics of 1.84% samples was above the threshold value. This shows that the PCA model in time domain can capture the major correlation and variance among the system variables.

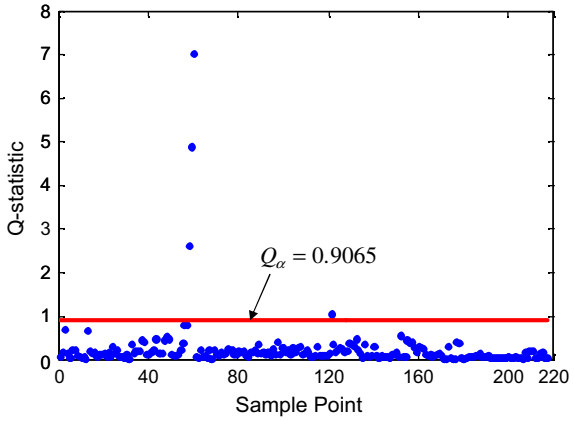

Fig. 5. Q-statistic plot of the conventional PCA model using training data.

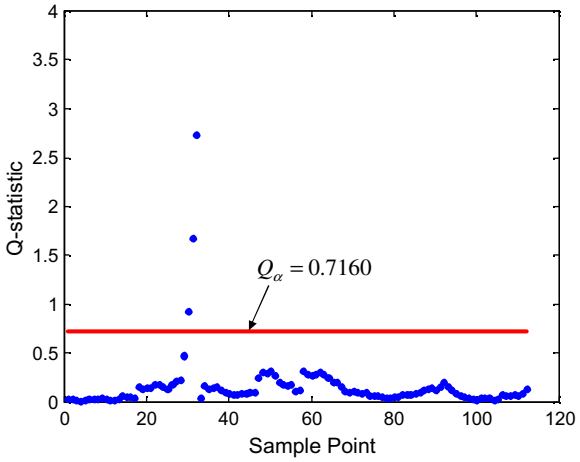

Fig. 6. Q-statistic plot of the wavelet–PCA model using training data.

For the training model of approximation coefficient matrix **B** using wavelet decomposition, 98.3% of the total variance of the system can be explained using three principal components corresponding to the three largest eigenvalues. These PCs were retained for the wavelet–PCA model. The Q-statistics plot of the wavelet–PCA model using the approximation coefficients decomposed from measurements in normal sensor conditions is presented in Fig. 6. The detection threshold of Q-statistics is 0.7160 also with the confidence level of 95%. The Q-statistics of 97.32% samples was within the threshold value. Only 2.68% of the total samples were abnormally above the threshold value. This means that the wavelet–PCA model can also describe the major correlation among the system measurements using wavelet transform.

4.4. Validation results and analysis

Many tests were conducted to evaluate the sensor FDD&E performance of the conventional PCA model using simply processing measurements directly and the performance of the wavelet–PCA model by adding biases of different magnitudes to the measurements for model validations. In these tests, only the sensors not used for feedback control were added with biases as it is impossible to simulate the real operation of the chiller system by simple adding a bias used in the feedback control loops without simulating its effects on the other variables. Therefore, biases were only added to the return cooling water temperature sensor (T_{cwr}), return chilled water temperature sensor (T_{chwr}), condensing temperature sensor (T_{cd}), evaporating temperature sensor (T_{ev}), condensing pressure transducer (P_{cd}), evaporating pressure transducer (P_{ev}), and power transducer (W_{comp}). Only one sensor was biased at a time.

In this study, detection ratio is used to describe the capability of fault detection using the PCA method. Detection ratio is the ratio of the number of samples whose Q-statistic values go beyond the threshold to the total number of samples used in a test. When the detection ratio is less than 20%, the fault is assumed to be not detected successfully (i.e., fail to detect the fault). Diagnosis ratio is used to describe the capability of fault isolation. Diagnosis ratio is the ratio of the number of samples which is successfully diagnosed to the number of samples whose Q-statistic values go beyond the threshold. When the diagnosis ratio is less than 50%, the fault is not isolated correctly (i.e., fail to diagnose the fault). Relative estimation error (Err) is used to describe the performance of measurement estimation, which is the ratio of the absolute difference between the estimated bias error and the added bias error to the added bias error. The estimated bias is the average value of the estimated biases of all the samples which were successfully diagnosed. The magnitudes of the biases added to measurements to generate the faulty data are to make the detection ratio range from 100% to less 20%.

Table 1 presents the detailed performance of fault detection, fault diagnosis and measurement estimation (recovery) using the conventional PCA model and the wavelet–PCA model on the fault biases on return cooling water temperature sensor (T_{cwr}), return chilled water temperature sensor (T_{chwr}), condensing temperature sensor (T_{cd}), and evaporating temperature sensor (T_{ev}). As far as the fault FDD&E on the biases of T_{cwr} is of concern, the detectable bias using the PCA model was about 1.0 °C, and the diagnosable bias is about 1.2 °C. However, when the wavelet–PCA model was used, the detectable bias could be low to 0.6 °C with the detection ratio about 34.68% although it failed to isolate where the fault was.

At the same bias magnitude, the wavelet–PCA model can detect and diagnose the faulty sensor and recover the measurements much better than the conventional PCA model does, which uses simple processing measurements in time domain directly. Fig. 7 schematically presents the Q-statistic plot of the conventional PCA model using faulty return cooling water temperature T_{cwr}, where the bias was 1.2 °C. Only 35.39% of the samples was detected to be faulty above the threshold ($Q_\alpha = 0.9065$). At the same time, the fault almost failed to be isolated successfully with the diagnosis ratio of 53.4%. The bias estimation error was also high (12.74%). When wavelet transform was used to extract approximation coefficients from the original samples for modeling and validation, the performance of FDD&E using PCA analysis was improved greatly. The significant improvement is illustrated as Fig. 8 using the wavelet–PCA model. The total samples were detected faulty far from the threshold ($Q_\alpha = 0.7160$) when the bias of return cooling water temperature T_{cwr} was 1.2 °C. The diagnosis ratio was also improved to 80.35% comparing to 53.49% using the conventional PCA model. The estimated bias (1.24 °C) was also much close to the added bias (1.2 °C) as shown in Table 1.

The FDD&E on the bias faults of temperatures T_{chwr}, T_{cd}, and T_{ev} also demonstrated the same results as shown in Table 1. It is worth to point out that both the conventional PCA model and wavelet–PCA model have higher resolution of detection and diagnosis on chilled water

Table 1
Comparison of FDD&E performance on temperature sensor faults using the conventional PCA model and the wavelet–PCA model

	PCA model in time domain					Wavelet–PCA model (level 3)			
	Bias	Detection ratio (%)	Diagnosis ratio (%)	Estimated	Err (%)	Detection ratio (%)	Diagnosis ratio (%)	Estimated	Err (%)
T_{cwr} (°C)	2.0	100	96.71	1.98	1.02	100	98.84	1.99	0.40
	1.5	84.36	92.68	1.52	1.34	100	98.27	1.49	0.37
	1.4	62.96	87.58	1.46	3.99	100	97.11	1.40	0.16
	1.3	43.21	73.33	1.39	6.91	100	89.60	1.31	1.05
	1.2	*35.39*	*53.49*	*1.35*	*12.74*	*100*	*80.35*	*1.24*	*3.50*
	1.1	27.16	Failed	–	–	100	73.41	1.17	5.99
	1.0	22.63	Failed	–	–	100	71.68	1.07	7.08
	0.7	Failed	–	–	–	78.61	57.35	0.89	27.77
	0.6	Failed	–	–	–	34.68	Failed	–	–
T_{chwr} (°C)	2.0	100	100	2.09	4.47	100	100	2.12	5.75
	1.5	100	100	1.59	5.95	100	100	1.62	7.67
	1.0	99.18	98.76	1.10	9.60	100	100	1.12	11.50
	0.7	68.72	95.21	0.88	26.06	99.42	100	0.82	16.73
	0.5	41.15	87.00	0.78	55.94	86.13	100	0.66	31.64
	0.4	30.45	81.08	0.71	78.38	74.57	100	0.58	46.00
	0.3	Failed	–	–		52.60	100	0.52	73.43
T_{ev} (°C)	2.0	100	100	1.94	3.09	100	100	1.94	3.17
	1.5	100	100	1.44	4.11	100	100	1.44	4.23
	1.0	100	100	0.94	6.17	100	100	0.94	6.34
	0.5	99.59	96.28	0.44	11.28	100	100	0.44	12.68
	0.4	97.53	91.98	0.35	12.28	100	100	0.34	15.85
	0.3	48.94	75.63	0.29	4.03	99.42	91.86	0.24	20.20
	0.2	Failed	–	–	–	36.41	Failed	–	–
T_{ed} (°C)	2.0	74.07	90.56	1.91	4.59	100	98.27	1.90	4.95
	1.7	40.33	73.47	1.61	5.07	100	96.53	1.60	5.73
	1.6	33.74	60.98	1.53	4.52	100	93.06	1.51	5.86
	1.5	27.16	37.88	1.43	4.53	100	90.75	1.41	6.21
	1.4	23.05	Failed	–	–	100	88.44	1.31	6.62
	1.3	20.58	Failed	–	–	89.02	84.42	1.21	7.02
	1.2	Failed	–	–	–	70.52	72.13	1.11	7.13
	1.1	Failed	–	–	–	50.29	Failed	–	–
	1.0	Failed	–	–	–	40.46	Failed	–	–

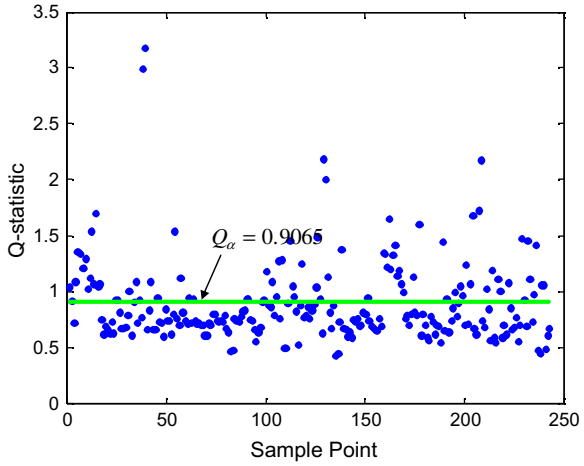

Fig. 7. Q-statistic plot of the conventional PCA model using faulty T_{chwr} (bias + 1.2).

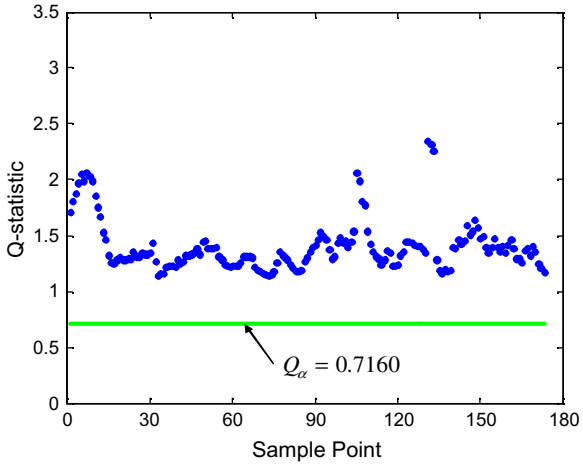

Fig. 8. Q-statistic plot of the wavelet–PCA model using faulty T_{chwr} (bias + 1.2).

temperature (T_{chwr}) faults and evaporating temperature (T_{ev}) faults than cooling water temperature (T_{cwr}) faults and condensing temperature (T_{cd}) faults.

The detailed performance of FDD&E using the conventional PCA model and the wavelet–PCA model on the fault biases on pressure transducers (P_{ev} and P_{cd}) and power

Table 2
Comparison of FDD&E performance on pressure transducer faults and power transducer faults using the conventional PCA model and the wavelet–PCA model

	Conventional PCA model					Wavelet–PCA model (Level 3)			
	Bias	Detection ratio (%)	Diagnosis ratio (%)	Estimated	Err (%)	Detection ratio (%)	Diagnosis ratio (%)	Estimated	Err (%)
P_{ev} (kPa)	20.0	100	100	19.35	3.25	100	100	19.51	2.45
	10.0	100	98.35	9.36	6.40	100	100	9.51	4.90
	5.0	63.37	70.13	5.00	0.00	100	98.84	4.52	9.60
	4.0	27.16	Failed	–	–	97.69	84.62	3.59	10.26
	3.0	Failed	–	–	–	43.93	Failed	–	–
	2.0	Failed	–	–	–	32.37	Failed	–	–
P_{cd} (kPa)	80.0	100	97.53	76.43	4.46	100	100.00	76.02	4.98
	70.0	72.84	92.66	67.21	3.99	100	98.84	66.02	5.69
	60.0	45.68	76.58	57.48	4.20	100	97.11	56.07	6.55
	50.0	24.69	Failed	–	–	96.53	88.62	46.24	7.52
	40.0	Failed	–	–	–	56.07	56.70	37.44	6.40
	30.0	Failed	–	–	–	35.84	Failed	–	–
	20.0	Failed	–	–	–	31.32	Failed	–	–
W_{comp} (kW)	100	91.77	98.65	112.26	12.26	100	100	111.17	11.17
	90	75.72	97.83	106.62	18.47	100	100	101.17	12.41
	80	59.67	96.55	101.50	26.88	100	100	91.17	13.96
	70	51.44	93.60	94.69	35.27	100	100	81.17	15.96
	60	42.39	89.32	87.3	45.5	98.27	100	71.48	19.13
	50	31.69	76.62	82.02	64.04	73.41	100	66.15	32.30
	40	24.28	61.02	74.81	87.025	45.66	100	65.20	63.00
	30	Failed	–	–	–	41.62	100	56.97	89.90
	20	Failed	–	–	–	38.73	67.16	47.37	136.85
	10	Failed	–	–	–	31.21	Failed	–	–

transducer (W_{comp}) is presented in Table 2. The detectable bias of P_{ev} is about 4.0 kPa using the conventional PCA model while the detectable bias is about 2.0 kPa using the wavelet–PCA model. The capability of fault diagnosis using the wavelet–PCA model was also higher than that using the conventional PCA model at the same fault magnitudes. When comparing the FDD&E performance on P_{ev} and P_{cd} faults using both models, both models are more sensitive on P_{ev} faults than on P_{cd} faults. The detectable bias and diagnosable bias of P_{cd} faults using the wavelet–PCA model were about 20 and 40 kPa, respectively, in this study. As for the electricity power, the relative errors of estimation of introduced biases to the power transducer were much larger than that of the other sensor biases, whose relative estimation errors were mostly lower than 10%. This might be explained as follows. The electrical power input is, to a great extent, affected by variables, such as water temperatures and flow rates, and tends to experience a wider range of variations when comparing with these other variables. Therefore, if there is a bias error with the measurement of the electrical power input, it is more difficult for the FDD&E strategy to accurately estimate the magnitude of this bias. However, in practical applications, the measurement of electrical power is much more accurate and reliable compared with other thermal variables such as temperatures and pressures. In this regard, the main concerns should be on the monitoring and FDD&E of the thermal physical measurements.

It can be concluded that the wavelet–PCA-based chiller sensor FDD&E strategy has better performance of fault detection, fault diagnosis and fault estimation than the strategy using the conventional PCA model. In the conventional PCA model, the measurements after outlier filtering and simple steady-state filtering are used for modeling and validation. In fact, only the data of significant dynamics is ruled out. There are still a lot of noises and obvious dynamics embodied in the remained data. These noises and dynamics severely deteriorate the FDD&E performance using the PCA method. Wavelet transform can extract the approximations of these measurements by separating the noises and obvious dynamics. These approximation coefficients are used for PCA modeling and validation to improve the FDD&E performance using principal component analysis.

The FDD&E performances of the wavelet–PCA models using the wavelet decomposition at different levels were also investigated. Table 3 presents the detailed performances of FDD&E of wavelet models using different levels

Table 3
Comparison of FDD&E performance on the sensor fault using wavelet–PCA models at different level decomposition (T_{chwr} bias + 1.3)

	Detection ratio (%)	Diagnosis ratio (%)	Estimated	Err (%)
Level 1 wavelet–PCA model	15.67 (Failed)	–	–	–
Level 2 wavelet–PCA model	81.17	54.64	1.25	4.19
Level 3 wavelet–PCA model	100	89.60	1.31	1.05

of decomposition, i.e., level 1, level 2, and level 3. The results show that the wavelet–PCA model using a high level decomposition had better performance than that using a low level decomposition. Of course, at least two points should be considered when determining as to which level wavelet decomposition is used. One is the computation cost of DWT and inverse DWT. The other is that enough samples are obtained to meet the length requirement of discrete wavelet transform and enough approximation coefficients for PCA modeling after wavelet decomposition.

5. Conclusion

Reliability and accuracy of sensor measurements are essentially important for chiller performance monitoring, energy efficiency, fault diagnosis and optimal control of chiller plants. An enhanced sensor fault detection, diagnosis and estimation strategy using wavelet analysis and principal component analysis is developed and presented. The test results using the field operation data demonstrated that this strategy is more effective and reliable to detect and diagnose and estimate sensor faults when compared with conventional PCA-based strategy, which directly employs raw measurements or operation data after simple processing. At the same magnitudes of sensor faults, the wavelet–PCA-based strategy can improve the detection ratio and diagnosis ratio significantly and improve the estimation accuracy obviously as well. The wavelet–PCA-based strategy can also detect and diagnose sensor faults at small magnitudes while conventional PCA-based strategy fails. The performances of FDD&E of wavelet–PCA models using different level decomposition were also investigated.

Principal component analysis provides a good means of generating useful residuals for sensor-fault detection and diagnosis and estimation. However, using raw measurements or operation data after simple processing directly for PCA modeling deteriorates these useful residuals preventing effective sensor fault detection, diagnosis and estimation. The reason is that these data still embody obvious noises and dynamics covering the effects of sensor faults. Wavelet analysis can separate these noises and dynamics from raw data by representing with approximation coefficients. Using these approximation coefficients for PCA modeling can enhance the performance of PCA for sensor fault detection and diagnosis and estimation. The wavelet–PCA-based FDD&E strategy is robust in that it is capable of processing noises and dynamics and it can capture the systematic variations of chiller systems.

Acknowledgements

The search presented in this paper was financially supported by a grant of the Research Grants Council (RGC) of the Hong Kong SAR.

References

[1] J.E Braun, Methodologies for the design and control of central cooling plant, PhD Thesis, University of Wisconsin, Madison, 1988.
[2] S.H. Cao, J.C. Cao, Forecast of solar irradiance using recurrent neural networks combined with wavelet analysis, Applied Thermal Engineering 25 (2–3) (2005) 161–172.
[3] K.T. Chan, F.W. Yu, Applying condensing-temperature control in air-cooled reciprocating water chillers for energy efficiency, Applied Energy 72 (3–4) (2002) 565–581.
[4] Y.C. Chang, F.A. Lin, C.H. Lin, Optimal chiller sequencing by branch and bound method for saving energy, Energy Conversion and Management 46 (12–14) (2005) 2158–2172.
[5] Y.M. Chen, X.L. Hao, G.Q. Zhang, et al., Flow meter fault isolation in building central chilling systems using wavelet analysis, Energy Conversion and Management 47 (13–14) (2006) 1700–1710.
[6] T.T. Chow, G.Q. Zhang, Z. Lin, et al., Global optimization of absorption chiller system by genetic algorithm and neural network, Energy and Buildings 34 (1) (2002) 103–109.
[7] D. Clarke, Intelligent instrumentation, Transactions of the Institute of Measurement and Control 22 (1) (2000) 3–27.
[8] J. Cui, S.W. Wang, A model-based online fault detection and diagnosis strategy for centrifugal chiller systems, International Journal of Thermal Science 44 (10) (2005) 986–999.
[9] H. Ding, J.H. Liu, Z.R. Shen, Drift reduction of gas sensor by wavelet and principal component analysis, Sensors and Actuators B: Chemical 96 (1–2) (2003) 354–363.
[10] R. Dorr, F. Kratz, J. Ragot, et al., Detection, isolation, and identification of sensor faults in nuclear power plants, IEEE Transactions on Control System Technology 5 (1) (1997) 42–60.
[11] L.N. Grace, D. Datta, S.A. Tassou, Sensitivity of refrigeration system performance to charge levels and parameters for on-line leak detection, Applied Thermal Engineering 25 (4) (2005) 557–566.
[12] H. Grimmelius, J. Woud, G. Been, On-line failure diagnosis for compression refrigeration plants, International Journal of Refrigeration 18 (1) (1995) 31–41.
[13] J.E. Jackson, A User's Guide to Principal Components, John Wiley & Sons, 1991.
[14] Y.Z. Jia, T. Reddy, Characteristic physical parameter approach to modeling chillers suitable for fault detection, diagnosis, and evaluation, Journal of Solar Energy Engineering, Transactions of the ASME 125 (3) (2003) 258–265.
[15] X.Q. Jin, Z.M. Du, Fault tolerant control of outdoor air and AHU supply air temperature in VAV air conditioning systems using PCA method, Applied Thermal Engineering 26 (11–12) (2006) 1226–1237.
[16] W.Y. Lee, J.M. House, N.H. Kyong, Subsystem level fault diagnosis of a building's air-handling unit using general regression neural networks, Applied Energy 77 (2) (2004) 153–170.
[17] R. Mah, A. Tamhane, Detection of gross errors in process data, AIChE Journal 28 (5) (1982) 828–830.
[18] Pacific Gas and Electric, CoolTools: A Toolkit to Optimize Chilled Water Plants, San Francisco, CA, 2001.
[19] D. Richard, F. Kratz, J. Ragot, et al., Detection, isolation, and identification of sensor faults in nuclear power plants, IEEE Transactions on Control System Technology 5 (1) (1997) 42–60.
[20] T. Rossi, Detection, diagnosis, and evaluation of fault in vapor compressor cycle equipment, Ph.D. Thesis, Purdue University, 1995, 205pp.
[21] T. Rossi, J. Braun, A statistical, rule-based fault detection and diagnostic method for vapor compression air conditioners, International Journal of HVAC&R Research 3 (1) (1997) 19–37.
[22] E. Russell, Data-driven Techniques for Fault Detection and Diagnosis in Chemical Process, Springer, 2000.
[23] G. Strang, Wavelet transforms versus Fourier transforms, Bulletin of the American Mathematical Society 28 (1993) 288–305.

[24] M. Stylianou, Application of classification functions to chiller fault detection and diagnosis, ASHRAE Transactions 103 (1) (1997) 645–656.
[25] D.J. Swider, M.W. Browne, P.K. Bansal, et al., Modelling of vapour-compression liquid chillers with neural networks, Applied Thermal Engineering 21 (3) (2001) 311–329.
[26] S.W. Wang, J.B. Wang, Law-based sensor fault diagnosis and validation for building air-conditioning systems, HVAC&R Research 5 (4) (1999) 353–380.
[27] S.W. Wang, F. Xiao, Sensor fault detection and diagnosis of air-handling units using a condition-based adaptive statistical method, HVAC&R Research 12 (1) (2006) 127–150.
[28] S.W. Wang, J. Burnett, Online adaptive control for optimizing variable-speed pumps of indirect water-cooled chilling systems, Applied Thermal Engineering 21 (11) (2001) 1083–1103.
[29] S.W. Wang, J.Y. Qin, Sensor fault detection and validation of VAV terminals in air conditioning systems, Energy Conversion and Management 46 (15–16) (2005) 2482–2500.
[30] S.W. Wang, J.T. Cui, Sensor-fault detection, diagnosis and estimation for centrifugal chiller systems using principal-component analysis method, Applied Energy 82 (3) (2005) 197–213.
[31] D. Wang, J.A. Romagnoli, Robust multi-scale principal components analysis with applications to process monitoring, Journal of Process Control 15 (8) (2005) 869–882.
[32] H. Yoshida, T. Ivami, H. Yuzawa, et al., Typical faults of air conditioning systems and fault detection by ARX model and extended Kalman filter, ASHRAE Transactions 102 (1) (1996) 557–564.
[33] M. Zuppa, C. Distante, Persaud, et al., Recovery of drifting sensor response by means of DWT analysis, Sensors and Actuators B: Chemical 120 (2) (2007) 411–416.